AFRL-SR-AR-TR-05-

0498

REPORT DOCUMENTATION PAGE

1. REPORT DATE *(DD-MM-YYYY)*	2. REPORT TYPE	3. DATES COVERED *(From - To)*
11-30-2005	FINAL	5/15/02 - 5/14/05

4. TITLE AND SUBTITLE
Fundamental Interface Structure-Property Relationships for High-Temperature Ceramic Composites

5a. CONTRACT NUMBER

5b. GRANT NUMBER
F49620-02-1-0211

5c. PROGRAM ELEMENT NUMBER

6. AUTHOR(S)
Elizabeth C. Dickey

5d. PROJECT NUMBER

5e. TASK NUMBER

5f. WORK UNIT NUMBER

7. PERFORMING ORGANIZATION NAME(S) AND ADDRESS(ES)

Robert Killoren
Associate Vice President for Research
The Pennsylvania State University
Office of Sponsored Programs
110 Technology Center Building
University Park, PA 16802-7000

8. PERFORMING ORGANIZATION REPORT NUMBER
424-36/776K

9. SPONSORING / MONITORING AGENCY NAME(S) AND ADDRESS(ES)

Carmelita B. Calvert, USAF,AFRL
GovProg Mgr-Dr.Joan Fuller,AFOSR NA
Air Force Off. of Scientific Research
4015 Wilson Boulevard, Room 713
Arlington, VA 22203-1954

Office of Naval Research
Chicago Regional Office
536 South Clark Street, Room 286
Chicago, IL 60605-1588

10. SPONSOR/MONITOR'S ACRONYM(S)

11. SPONSOR/MONITOR'S REPORT NUMBER(S)

12. DISTRIBUTION / AVAILABILITY STATEMENT
Approved for public release; distribution is unlimited.

13. SUPPLEMENTARY NOTES

14. ABSTRACT
This research program focused on studying interface structure and thermal compatibility stresses in several directionally solidified eutectic ceramic materials, which are candidates for high-temperature and ultra-high temperature structural materials in aerospace applications. Under this award we specifically investigated the alumina-zirconia and lanthanum hexaboride- zirconium diboride eutectic systems. High-resolution transmission electron microscopy was utilized to understand interfacial structures in these materials and x-ray diffraction was utilized to measure thermal residual stresses. A major conclusion of the research program was that thermal stresses are the dominant factor that leads to the high fracture toughness in the lanthanum hexaboride- zirconium diboride eutectic systems. The research program supported two Ph.D. students and two undergraduate students.

15. SUBJECT TERMS
ceramic composites, ultra high-temperature, alumina-zirconia, lanthanum-hexaboride, residual stress, interfaces, transmission electron microscopy, directional solidification

16. SECURITY CLASSIFICATION OF:			17. LIMITATION OF ABSTRACT	18. NUMBER OF PAGES	19a. NAME OF RESPONSIBLE PERSON
a. REPORT	b. ABSTRACT	c. THIS PAGE		12	Dr. Elizabeth Dickey
					19b. TELEPHONE NUMBER *(include area code)* 814-865-5067

FINAL REPORT

For

AFOSR AWARD # F49620-02-1-0211

FUNDAMENTAL STRUCTURE-PROPERTY RELATIONSHIPS FOR HIGH-TEMPERATURE CERAMIC COMPOSITES

Period
May 15, 2002 -- May 14, 2005

Elizabeth C. Dickey
Department of Materials Science and Engineering
The Pennsylvania State University

Abstract

Directionally-solidified ceramic eutectics show promise as high-temperature structural materials because of their high-temperature strength and, in some systems, creep resistance.[1-5] The focus of this research program has been to study fundamental interfacial issues in these composite materials that could influence or control mechanical behaviors. We have investigated two eutectic systems: Al_2O_3-$ZrO_2(Y_2O_3)$ and LaB_6-ZrB_2. The interfaces between the two constituent phases play a key role in several deformation mechanisms including fracture toughness and creep. Our goal has been to characterize the structure of these interfaces at the atomic length scale, which provides information about bonding across the interface. Furthermore, compatibility constraints at the internal interfaces can lead to residual stresses upon thermal cycling and elastic interaction stresses under applied loads.[6] The magnitudes and distributions of these stresses also have important ramifications for the mechanical behavior of the composites.

I. Objectives

This research program aims to elucidate fundamental aspects of interfacial bonding and interfacial compatibility stresses in high-temperature ceramic composites. The principal class of composite materials investigated is directionally solidified ceramic eutectics. To assess the relationship between interface structure, bonding and interfacial compatibility stresses in these classes of materials, this research aims to develop analytical techniques to probe the structure and strain state of the material from multiple length scales. First, the microstructure and crystallography of the composite are thoroughly characterized. Transmission electron microscopy is utilized study interface structure and associated defects. X-ray diffraction is employed to measure the strain tensors in each phase, which are subsequently converted to stress tensors.

II. Research Results

II.1 Al_2O_3-$ZrO_2(Y_2O_3)$ Directionally Solidified Eutectics (DSEs)

Following on from AFOSR award, F49620-99-1-0266, we completed work on the Al_2O_3-$ZrO_2(Y_2O_3)$ DSE. Fig. 1a is a micrograph showing the Al_2O_3 (white phase) distributed within the ZrO_2 matrix (black phase). As evidenced in the high-resolution transmission electron micrograph (HRTEM) in Fig. 1b, the interfaces between the two phases are highly crystalline and atomically abrupt.

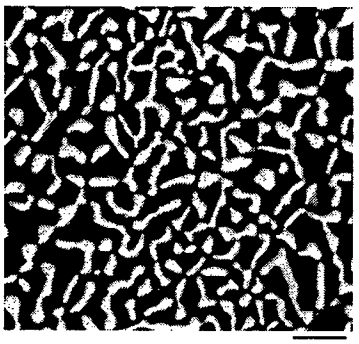

Fig. 1a SEM image of Al_2O_3-$ZrO_2(Y_2O_3)$ DSE.

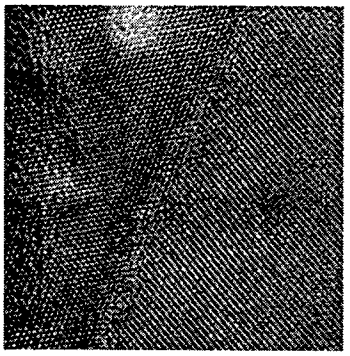

Figure 1b. HRTEM image of the Al_2O_3 (left) and $ZrO_2(Y_2O_3)$ (right) interface showing clean atomically abrupt interfaces.

Pole figures from Al_2O_3 and $ZrO_2(Y_2O_3)$ are shown in figures 2a and 2b, respectively. Whereas the Al_2O_3 is nearly single crystalline with [0001] oriented along the growth axis, the ZrO_2 has multiple orientations, although it is highly (220) textured along the growth axis.

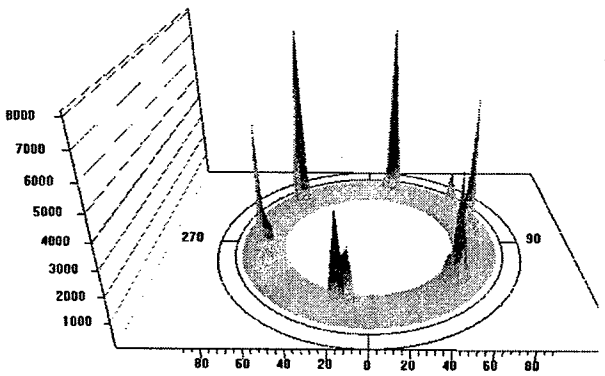

Figure 2a: (1123) pole figure of the Al_2O_3 phase in an Al_2O_3-ZrO_2 DSE. Since the phase is nearly single crystalline, a rotated single crystal stiffness tensor can be used.

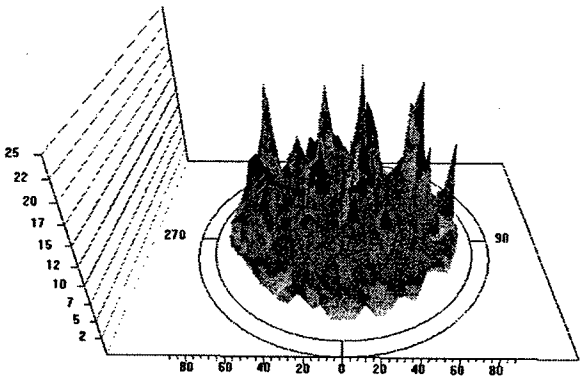

Figure 2b: (311) pole figure of the ZrO_2 phase in an Al_2O_3-ZrO_2 DSE. Since the phase is polycrystalline yet textured, a weighted stiffness tensor must be used.

Because the DSEs are highly textured, standard polycrystalline stress measurements using x-ray diffraction are not possible. It is therefore necessary to make measurements of interplanar spacings along particular sample directions where reflections are present. Once at least six interplanar-spacing measurements have been made and the unstressed lattice parameter measured, it is possible to fit the six components of the strain tensor to the experimental data. Typically, the system is over-determined by making at least twelve measurements and using a fitting routine to determine the strain tensor and error matrix.

The final step in the analysis is to convert the strain tensors to stress tensors with the stiffness tensors. Since the alumina is nearly single crystalline, the single-crystal stiffness tensor rotated to the correct reference frame can be used. The ZrO_2 phase, however, has much weaker texture and it is necessary to weight the stiffness tensor using the orientation distribution function (ODF) as outlined below:

406	105	105	0	0	0
105	406	105	0	0	0
105	105	406	0	0	0
0	0	0	55	0	0
0	0	0	0	55	0
0	0	0	0	0	55

Single crystal stiffness tensor of cubic ZrO_2 (MPa)

+ ODF

336	140	140	-2	-1	2
140	334	141	1	0	-1
140	141	334	0	1	-1
-2	1	0	91	-1	0
-1	0	1	-1	90	-2
2	-1	-1	0	-2	90

Weighted stiffness tensor (MPa)

Applying this procedure to Al_2O_3-ZrO_2(6.6wt% Y_2O_3) DSEs, the following stress tensors were determined where x_3 is normal to the growth axis:

Al_2O_3: | -364 32 56 / -454 -18 / -288 | +/- | 9 4 4 / 10 5 / 7 | (MPa)

ZrO_2: | 2280 -775 8 / 1586 -242 / 539 | +/- | 20 19 6 / 20 6 / 11 | (MPa)

The very large stresses, particularly in ZrO_2 which has a lower volume fraction, result from mismatches in thermal expansion/contraction between the two phases and the large temperature differential between the solidification temperature (~2180°C) and room temperature.

These stresses are actually low, only ~ 65% of those predicted from finite element modeling, assuming the stress-free temperature to be the eutectic temperature of 1880°C. These low stresses suggest that enough mobility was present during part of the cooling stage to prevent some residual stress accumulation. To understand if stress mitigation processes dynamically occur upon thermal cycling, we annealed the specimen at 1600°C for 5 hours and slowly cooled the specimen. Room temperature stresses were then remeasured, but showed no appreciable change.

Analogous stress measurements were made at elevated temperatures utilizing the domed hot-stage outfitted on a four-circle goniometer x-ray diffractometer as shown in Fig. 3.

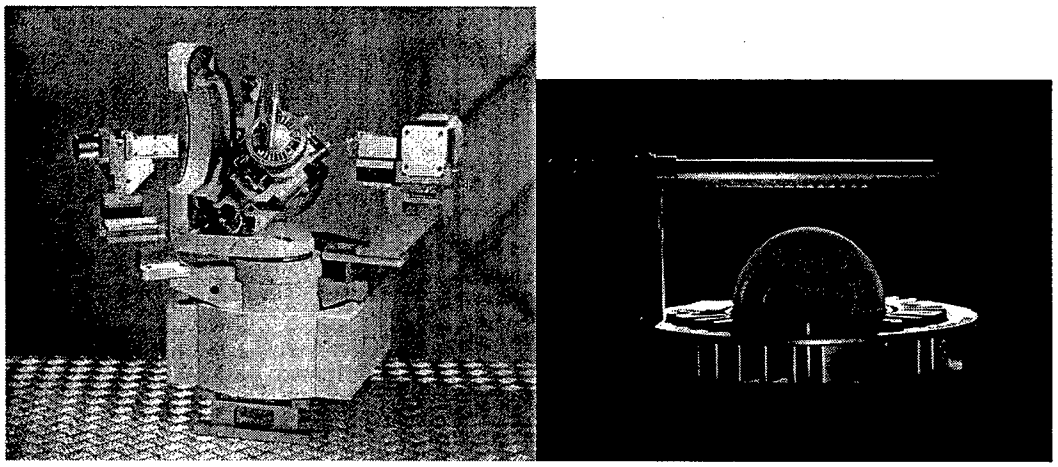

Fig. 3 a) four-circle goniometer Philips MRD x-ray outfitted with domed hot stage. b) close up of domed hot stage operated at 900°C.

Residual stress measurements were made at 400°C and 900°C. Loosely pressed powder specimens of Si (NIST standard) and Al_2O_3 were also measured at these temperatures for calibration purposes. The resulting stress tensors for Al_2O_3 are shown below:

Al_2O_3 (400°C):

$$\begin{vmatrix} -133 & 94 & -57 \\ & -26 & -0 \\ & & -116 \end{vmatrix} \quad +/- \quad \begin{vmatrix} 10 & 2 & 1 \\ & 13 & 4 \\ & & 7 \end{vmatrix} \quad \text{(MPa)}$$

Al_2O_3 (900°C):

$$\begin{vmatrix} 335 & 86 & -45 \\ & 427 & 0 \\ & & 409 \end{vmatrix} \quad +/- \quad \begin{vmatrix} 10 & 2 & 1 \\ & 13 & 4 \\ & & 7 \end{vmatrix} \quad \text{(MPa)}$$

As expected, the stresses decreased at 400°C to less that half of the room temperature values. At 900°C the Al_2O_3 went into tension indicating that the stress-free temperature is on the order of 500-600°C. So in service conditions of 1200-1400°C significant tensile stress will be present in the Al_2O_3.

II.2 LaB_6-ZrB_2 Directionally Solidified Eutectics

Figure 4 shows the typical microstructure of a LaB_6-ZrB_2 DSE boole grown at a rate of 6.0 mm/min in a 0.3 MPa argon atmosphere by collaborators at the Institute for Problems of Materials Sciences of Academy of Sciences of Ukraine. The ZrB_2 fibers (white phase) were uniform at the center of the rod (c), non-uniform at the edge (a), and were separated by several concentric circular matrix belts around the center (b). In the center or homogeneous area, the

average diameter of fibers was 0.6 μm. The volume fraction of the ZrB_2 phase was 18% as calculated by area fractions from digital micrographs taken from a transverse section at the center of the specimen (e.g. Fig. 1c); this coincides closely with that expected from the eutectic composition —17%.

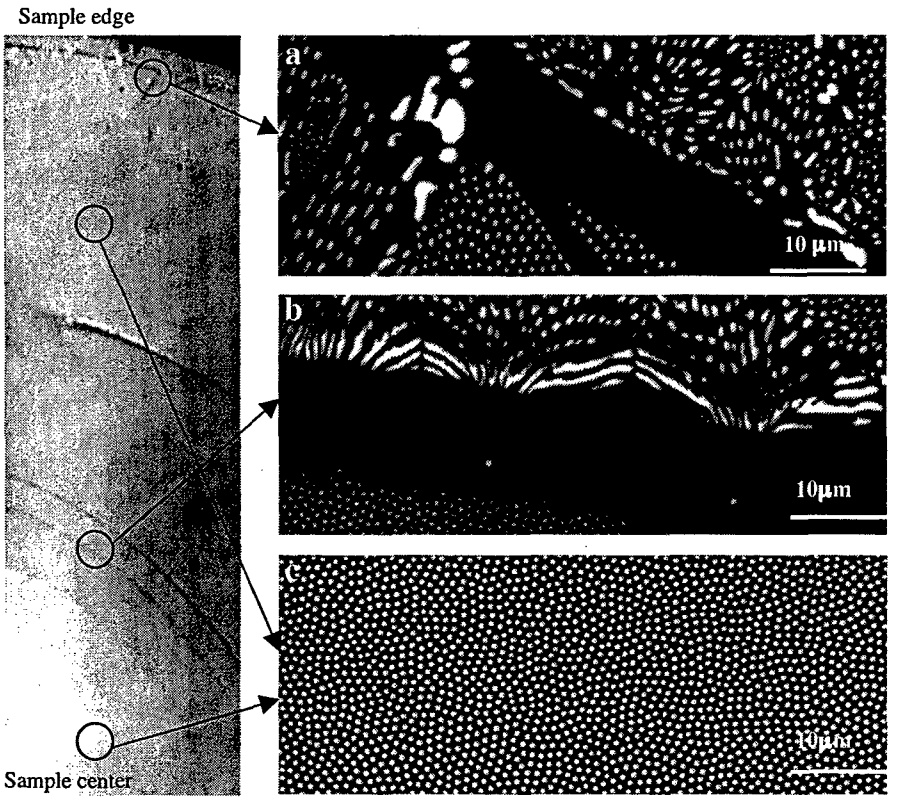

Figure 4: Optical microscopy images of LaB_6-ZrB_2 DSE. The growth of ZrB_2 fibers (white phase) is uniform at the center of the rod (c), non-uniform at the edge (a), and separated by several concentric circular matrix belts around the center (b).

Transmission electron microscopy (TEM) observations from the transverse-section specimens are summarized in Fig. 5. Figure 5g is an electron diffraction pattern, which confirms previous data that the [0001]-ZrB_2 was nominally parallel to the [001]-LaB_6 and (110)-LaB_6 paralleled (100)-ZrB_2. The intensity distributions apparent in Fig. 5c show that there was actually a 2.0° mistilt between the two [001] axes along the $[5\bar{2}0]$-LaB_6 direction. Furthermore, electron diffraction patterns a, b, e, f indicated that all of the fibers within the local area were oriented nominally the same with only about 0.02° deviation between the c-axes of different fibers. This result implies that the ZrB_2 phase was locally single crystalline in a 1 μm^2 area.

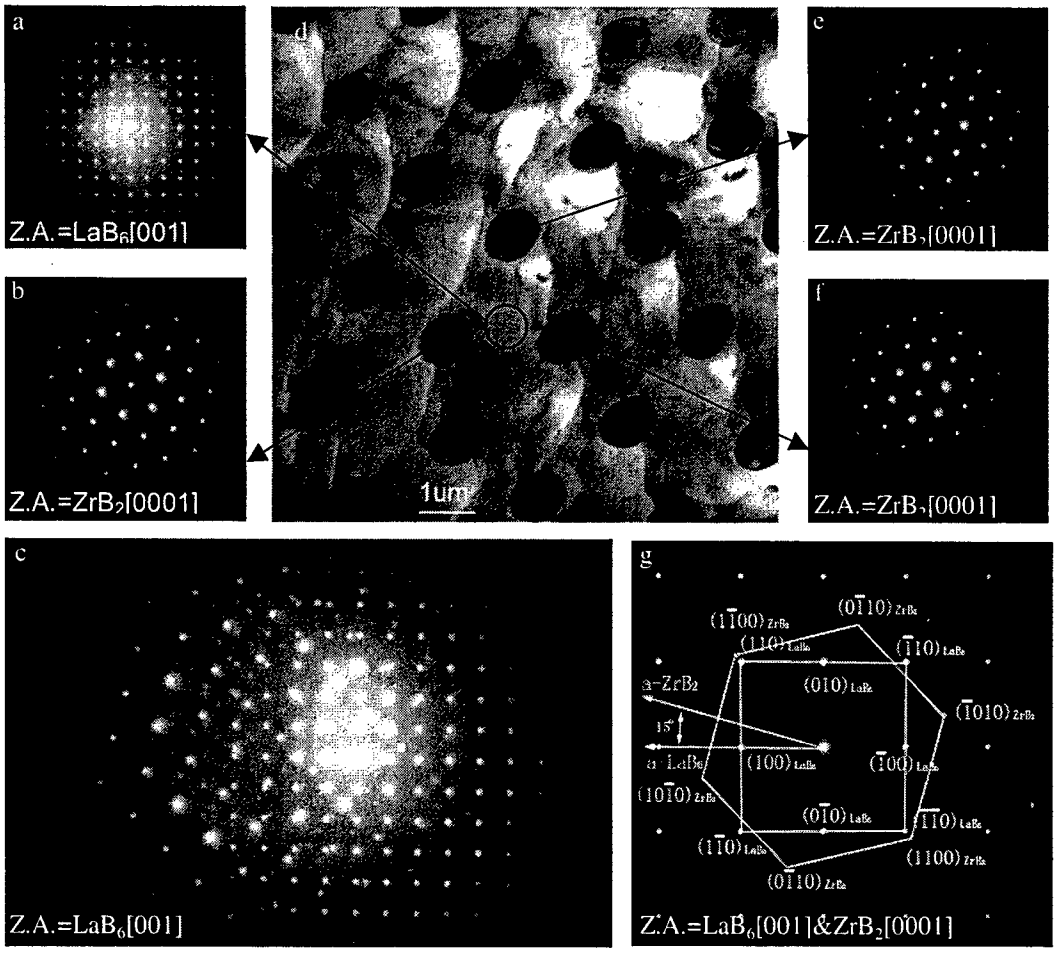

Figure 5: TEM data from the transverse section of a LaB_6-ZrB_2 DSE. g is the SAD pattern, which illustrates that the [0001] ZrB_2 is approximately parallel to [0001] LaB_6 and (110) LaB_6 parallels (1 $\bar{1}$ 00) ZrB_2. Intensity distributions in (c) show that there is actually a small misorientation between the two phases. Electron diffraction patterns from individual fibers (b, e, f) indicate that all of the LaB_6 fibers are locally oriented in the same direction within 0.02 degrees.

Table I summarizes the hardness and fracture toughness measurements via Vicker's indentation. The anisotropies of hardness and indentation fracture toughness were assessed by making measurements along different crystallographic directions on both transverse and longitudinal sections. Error bars were calculated from the standard deviation of six measurements. While the hardness did not vary appreciably between the two orientations, the fracture toughness was observed to be highly anisotropic. Toughening behavior was observed on longitudinal sections with crack deflection and bridging mechanisms apparent (see Figure 6). Cracks were difficult to initiate on transverse sections along directions perpendicular to the growth direction, but for 20N loads a fracture toughness of 11 $MPam^{1/2}$ could be measured.

Table I: Hardness and fracture toughness of LaB_6-ZrB_2 as measured from Vickers indentation.

	Transverse section		Longitudinal section	
	$[100]_{LaB_6}$	$[03\bar{2}]_{LaB_6}$	$[\bar{2}13]_{LaB_6}$	$[4\bar{2}3]_{LaB_6}$
Fracture toughness ($MPam^{1/2}$)	4.6±0.3	4.2±0.8	3.5±0.7	11.1±1.1
Hardness(GPa)	22.6±0.7		21.7±0.6	

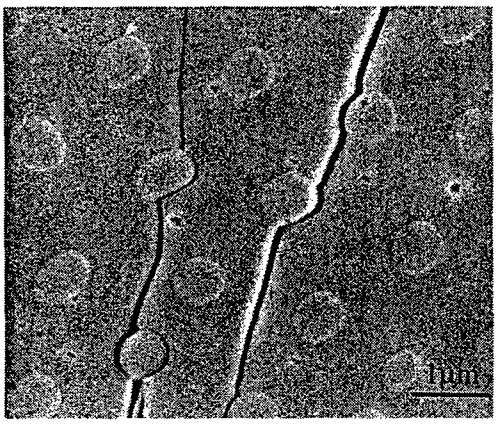

Figure 6a: SEM micrograph showing crack deflection along transverse sections.

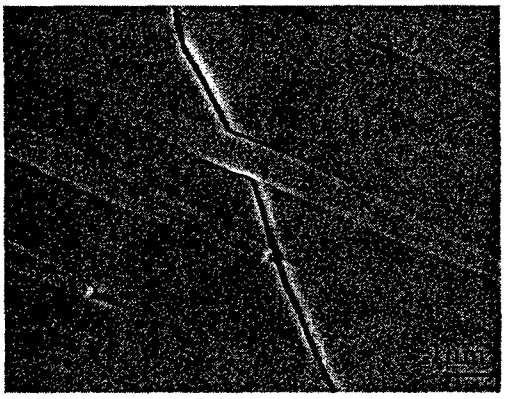

Figure 6b: SEM micrograph showing crack deflection and bridging along longitudinal sections.

The significant interface debonding observed in the LaB_6-ZrB_2 DSEs is intriguing, especially considering that these are very high-strength composites. We therefore performed more in-depth interface analysis to try to understand the origins of the debonding. TEM images of the LaB_6 fibers show significant faceting along particular crystallographic orientations. HRTEM images (Figure 7) show that the interfaces along these facets are atomically abrupt with no amorphous phases. The longest facets correspond to (110) LaB_6 //(11.0) ZrB_2. Indeed, this facet has the smallest two dimensional near-coincident site lattice (NCSL) with Γ=1 for the Σ_{LaB6}=6 NCSL. These observations suggest that the interfaces adopt thermodynamically low-energy orientations during the solidification process and would therefore be expected to be well-bonded. This is inconsistent with the observed crack deflection observations (Figure 6).

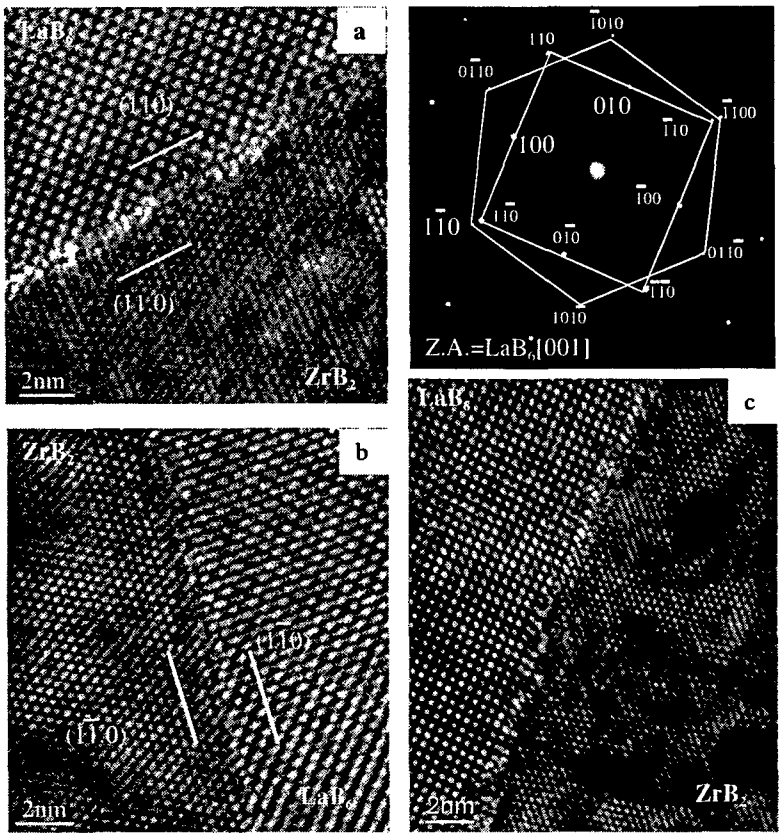

Figure 7: HRTEM images of interfaces on the transverse section. (a) is (110) LaB_6 //(11.0) ZrB_2 facet, (b) is (110) LaB_6 //(11.0) ZrB_2 facet and (c) is the stepped interface off the facet orientation.

Another possible origin of the significant interface debonding may be the residual stresses in the composite arising from the thermal expansion mismatches between the two phases. We have employed x-ray diffraction methods, as described above, to measure the room-temperature residual stresses. Members of a family of equivalent reflections were employed in order to

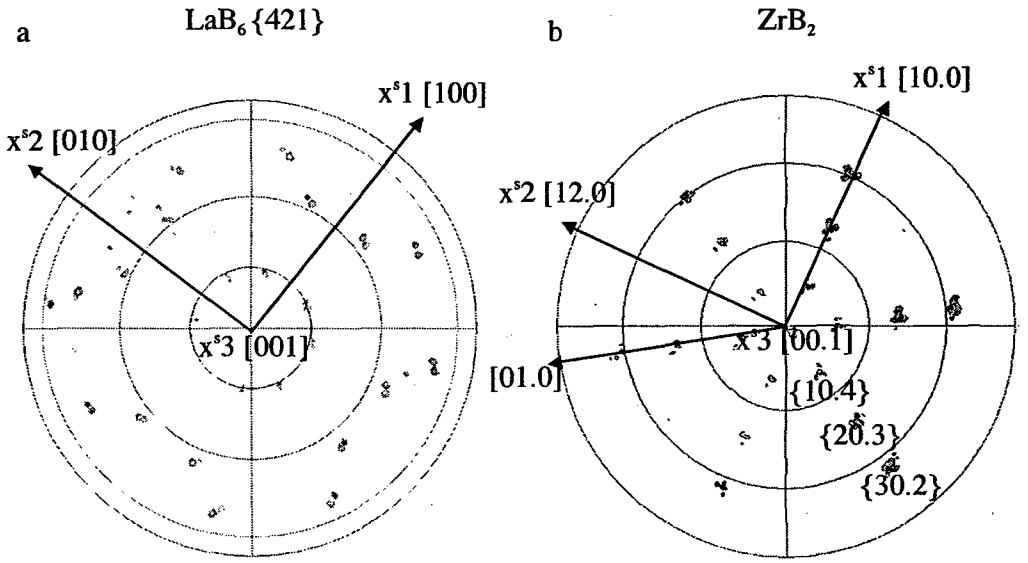

Fig. 8 Reflections used for strain measurements are a) {421} planes of LaB_6 and b) {10.4}, {20.3} and {30.2} planes of ZrB_2.

minimize the measurement error. Reflections with high diffraction angles were selected to maximize angular resolution. The stereographic projection of the reflections chosen for strain measurements are shown in Fig. 8. Samples were mounted on the goniometer so that the highest symmetry orientations of both phases ([001]-LaB_6 and [00.1]-ZrB_2) were located in the X-ray source-detector plane.

Measuring interplanar spacing from each of these reflections, the fundamental strain tensor was fitted. These residual strain tensors were then converted to stress tensors using published single crystal stiffness tensors rotated to the appropriate reference frame. The experimentally measured tensors are shown below for a eutectic crystal grown at 1mm/hr.

$$\sigma_{ZrB_2} = \begin{bmatrix} 728.7 & 19.93 & -31.2 \\ 19.93 & 665.3 & -221.8 \\ -31.2 & -221.8 & 482.4 \end{bmatrix} \pm \begin{bmatrix} 241.3 & 164.0 & 99.50 \\ 164.0 & 237.4 & 101.0 \\ 99.50 & 101.0 & 150.2 \end{bmatrix} MPa$$

$$\sigma_{LaB_6} = \begin{bmatrix} -125.0 & 27.39 & 5.406 \\ 27.39 & -205.5 & 73.34 \\ 5.406 & 73.34 & -165.0 \end{bmatrix} \pm \begin{bmatrix} 27.04 & 7.748 & 8.109 \\ 7.748 & 26.93 & 8.469 \\ 8.109 & 8.469 & 27.7 \end{bmatrix} MPa$$

The signs of normal stresses are in agreement with that predicted from differences in thermal expansion behavior: ZrB_2 fibers, which have larger thermal expansion coefficients, contract more during cooling from the solidification temperature and remain in tension. It is believed that these very high residual stresses are the predominant driving force for the significant crack deflection that is observed during fracture toughness testing.

References

[1] T. Mah, T.A. Parthasarathy and L.E. Matson, "Processing and mechanical properties of Al_2O_3/Y_3Al_5O12 (YAG) eutectic composite," *Ceramic Engineering and Science Proceedings*, 11, 1617-27 (1990).

[2] T.A. Parthasarathy and T. Mah, "Creep behavior of an Al_2O_3-$Y_3Al_5O_{12}$ eutectic composite," *Ceramic Engineering and Science Proceedings*, 11, 1628-38 (1990).

[3] A. Sayir and L. E. Matson, "Growth and Characterization of Directionally Solidified $Al_2O_3/Y_3Al_5O_{12}$ (YAG) Eutectic Fibers," in HITEMP Review Vol. 1 NASA CP-10082, (1991) 83.1.

[4] A. Sayir, R. M. Dickerson, H. M. Yun, S. Heidger and L. E. Matson, "High Temperature Mechanical Properties of Directionally Solidified $Al_2O_3/Y_3Al_5O_{12}$(YAG) Eutectic Fibers," in HITEMP Review Vol. 1, NASA CP-10146, (1994) 74.1-74.18.

[5] S. C. Farmer, A. Sayir and P. O. Dickerson, "Mechanical and Microstructural Characterization of Directionally-Solidified Alumina-Zirconia Eutectic Fibers," in "Ceramic Matrix Composites-Advanced High-Temperature Structural Materials," eds., R. A Lowden, M. K. Ferber, J. R. Hellmann, K. K. Chawla, and S. G. DiPietro, Mat. Res. Soc. Proc., 365 (1995) 11.

[6] E.C. Dickey, C. S. Frazer, T.R. Watkins and C.R. Hubbard, "Residual Stresses in High Temperature Ceramic Eutectics," *Journal of the European Ceramic Society,* 19 (1999) 2503-2509.

Personnel Supported

This grant supported the research activities of the following people from 2002-2005:

Elizabeth C. Dickey	Associate Professor, Pennsylvania State University
Colleen S. Frazer	Ph.D., University of Kentucky (now at Sandia National Lab)
Hongqi Deng	Ph.D., The Pennsylvania State University (expected May 2006)
C. Evan Jones	Undergraduate Student, Pennsylvania State University (now at University of Kentucky)
Jeffrey Bender	Undergraduate Student, Pennsylvania State University (now at the University of Virginia)

Publications resulting from grant

E.C. Dickey, C. S. Frazer, T.R. Watkins and C.R. Hubbard, "Residual Stresses in High Temperature Ceramic Eutectics," *Journal of the European Ceramic Society,* 19 (1999) 2503-2509.

C.S. Frazer, E.C. Dickey, and A. Sayir, "Crystallographic Texture and Orientation Variants in $Al_2O_3/Y_3Al_5O_{12}$ Directionally Solidified Eutectic Crystals," *J. Crystal Growth*, 233 (2001) 187-195.

C.S. Frazer, C.E. Jones, E.C. Dickey, "Interfacial Compatibility Stresses in Alumina-Zirconia and Alumina-YAG Composites," in Advances in Ceramic Matrix Composites VI, *Ceramic Transactions*, Volume 124 (2001) J.P. Singh, Narottam P. Bansal, and Ersan Ustundag, Editors, American Ceramic Society, Westerville, OH, pp.339-350.

"Directional Crystallization of Boride Eutectics," Yu.B. Paderno, V.N. Paderno, V.B. Filipov, A. Sayir, H. Deng, E.C. Dickey, *Journal of the European Ceramic Society,* in press.

H. Deng, E. C. Dickey, Y. Paderno, V. Paderno and V. Filippov, "Interface Crystallography and Structure in LaB_6-ZrB_2 Directionally Solidified Eutectics," submitted to *Acta Materialia.*

H. Deng, E.C. Dickey, "Residual Stresses in LaB_6-ZrB_2 Directionally Solidified Eutectics," in preparation for the *Journal of the American Ceramic Society.*

Awards Received

John T. Ryan Jr. Faculty Fellow, Pennsylvania State University 2005-2008 (for E.C. Dickey)